

STUDY OF SINGLE WIRE SCANNER MONITOR FOR FETS-FFA TEST RING

E. Yamakawa*, D. W. Posthuma de Boer, S. Machida, A. Pertica, A. Letchford

Rutherford Appleton Laboratory, Didcot, United Kingdom

Y. Ishi, T. Uesugi

Kyoto University Institute for Integrated Radiation and Nuclear Science, Osaka, Japan

Abstract

To confirm the use of Fixed Field Alternating gradient accelerator (FFA) as a high power pulsed neutron spallation source, a prototype called FETS-FFA is studied at Rutherford Laboratory (RAL). A single Wire Scanner Monitor (WSM) is planned to be used to measure beam position and beam profile in the ring. One of the concerns of this monitor is the thermal damage on the Carbon Nano Tube (CNT) wire due to high energy deposition of low energy proton beam in FETS-FFA (3–12 MeV). Furthermore, to measure a beam profile during beam acceleration in the ring, a diameter of CNT wire needs to be smaller than the orbit displacements in turns. To confirm whether a single WSM is suitable for FETS-FFA ring, two different beam tests were performed at RAL and at the Institute for Integrated Radiation and Nuclear Science, Kyoto University (KURNS). Both measurements demonstrated that the single WSM is applicable for FETS-FFA ring if the diameter of CNT is smaller than the orbit separation between two consecutive turns. In this paper, the detail of the design study of single WSM as well as the performance tests are presented.

INTRODUCTION

The ISIS-II project [1] is currently considering a 1.25 MW proton driver for a new pulsed spallation neutron source in Europe. A Fixed Field Alternating Gradient (FFA) ring [2, 3] is one option for the main ring of ISIS-II. In order to demonstrate that FFAs can provide the reliability required for user operations in ISIS-II, the small-scale Front End Test Stand and Fixed Field Alternating gradient (FETS-FFA) ring will be built by 2029. The baseline optics of the horizontal excursion FETS-FFA (hFFA) ring were recently finalised, and its main parameters are presented in Table 1.

Based on the planned commissioning scenario, a single WSM will be used to identify the beam profile and the beam position of the injected beam to optimize any injection mismatch with the design orbit and the Twiss parameters. Destructive monitors are extremely useful when a non-destructive monitor cannot detect the beam induced signal in the case of low intensity beam at the beginning of the beam commissioning. According to the measurement of the accelerating multi-turn beam profile in the FETS-FFA ring, the single WSM will be placed on the orbit of a certain beam energy. As the orbit radius changes with beam energy, a single stationary wire can measure the profile by intercepting the beam over several turns during an acceleration cycle.

Table 1: Parameters of 4-fold Symmetry FD-spiral FETS-FFA Ring in 2023

Parameter	Value
Beam energy range	3–12 MeV
Bunch intensity	3×10^{11} ppp
Repetition rate	100 Hz (50 pps)
Injection rate	50 Hz
RF frequency bandwidth	2–4 MHz
Harmonic number	2
Normalised Beam Core	10π mm mrad
Beam Size	± 20 mm
Orbit Excursion	600 mm
Vertical Physical Acceptance	± 32 mm

As the beam energy changes during a profile measurement, adiabatic damping will cause the transverse beam size to reduce on each successive turn. Furthermore, beam loss due to scattering at the wire might distort the profile during a measurement. To investigate whether the monitor can measure the beam profile in the FETS-FFA ring, a feasibility study of the single WSM is performed in this paper. This will include the relationship between wire thickness and turn separation, as well as predictions for wire heating. Profile measurements made at the FETS Linac and KURNS hFFA ring will then be shown and used to inform conclusions.

FEASIBILITY STUDY

Carbon Nano Tube (CNT) [4–6] wires are used for the single WSM in the FETS-FFA ring owing to their high melting temperature (3000 °C) and high tensile strength (1 GPa).

Wire Thickness

For the case of profile measurement of an accelerating beam over several turns in the FETS-FFA, separation between subsequent transverse profile samples will be fixed by the change in orbit displacement, as illustrated in Fig. 1. This will depend on the RF program and is not expected to be constant throughout an acceleration cycle. To investigate the impact of wire thickness on the measured beam profile, a computer simulation was performed with the vertical excursion FFA (vFFA) lattice [7, 8]¹. In the simulation,

¹ The lattice design of the FETS-FFA ring (Table 1) was changed from the vFFA to the horizontal excursion FFA (hFFA) in 2022. The lattice design of hFFA is different from that of vFFA, however the orbit displacements and the RF program are similar

injected particles were generated with a Gaussian distribution and transported using 4×4 transfer matrices with Py-TRACK [9]. Although the scattering angle and energy loss of particles at the wire were not taken into account in this calculation, the calculation stopped when a particle hit the wire, assuming 100 % beam-loss due to scatterings. The wire was placed at 3.41 MeV (averaged turn separation of 64.2 μm) and 10.95 MeV (averaged turn separation of 25.3 μm).

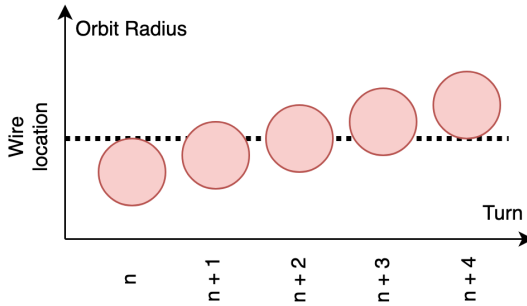


Figure 1: Schematic drawing of the profile measurement of an accelerating beam over several turns (red circles) in the FETS-FFA ring.

Figure 2 shows the computed beam profile measured by wires of differing thicknesses, at around 3 MeV and 12 MeV. In the case of 12 MeV, the beam size measured by each thickness of wire is consistent to the initial beam size of 12.7 mm. On the other hand, in the case of 3 MeV, a distortion can be seen when the wire thickness is larger than $\phi 30 \mu\text{m}$. Furthermore, the Root Mean Square (RMS) beam size is overestimated compared to the initial beam size of 17.1 mm. This is thought to be caused by the change in particle population throughout the simulation. Whilst the distortion is affected by the assumed loss due to scattering, these results are indicative of a more general relationship between profile accuracy and wire thickness. A beam which intercepts less material will be scattered less, which is particularly significant for the proposed multi-turn profile measurement. Ensuring that the wire thickness is less than the turn separation can help to limit the number of consecutive scattering events, and thus give a more accurate profile. The signal strength from the wire is expected to be proportional to the cross-section of the wire, and affects a Signal to Noise Ratio (SNR) and signal sensitivity of the wire. The thickness of the wire should be chosen with a reasonable balance between the SNR and profile distortion.

Heat Analysis

Temperature rise in the wire is an important consideration for all such interceptive diagnostics, but especially so when measuring the beam profile over multiple turns. The cumulative interaction period will be significantly longer than that of one-pass measurement. A heat analysis has therefore performed by the analytical simulation code [10] which computes a temperature change in the material. According to the vFFA beam parameters and its RF acceleration scheme, the

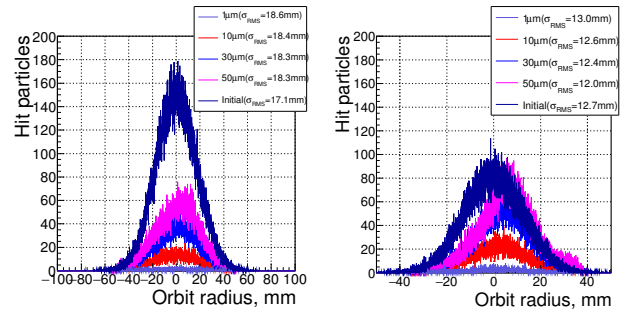


Figure 2: Computed beam profile with several thicknesses of CNTs at around 3 MeV (left) and 12 MeV (right).

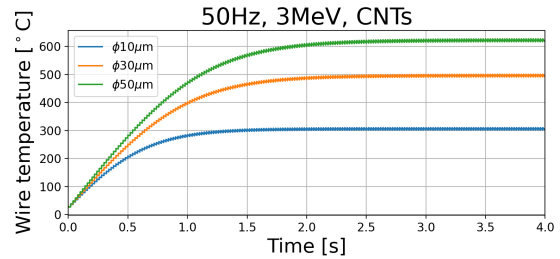


Figure 3: Transient temperature in each CNT wire. A thermal emissivity of CNT in vacuum is estimated to be 0.2 in this simulation.

time duration for the beam orbit to travel over the beam size ($2\sigma=8 \text{ mm}$) is 336 μs with harmonic number 2, corresponding to 0.143 mA of 3×10^{11} ppp, at injection beam energy of 3 MeV. As shown in Fig. 3, the steady temperature on each wire is below the CNT melting temperature.

Heat Test on FETS

To confirm whether a thin CNT wire is applicable with a 3 MeV proton beam, tests were performed with a 3 MeV H^- beam on the FETS Linac [11], using the ISIS single-wire injector profile monitor (SWIP) [12] (Fig. 4). Several diameters of CNT wires: $\phi 20$, $\phi 30$, $\phi 40$ and $\phi 50 \mu\text{m}$ were mounted on the monitor head. The monitor shaft is inclined at 44.5 degrees, and travels nearly 150 mm from the park position.

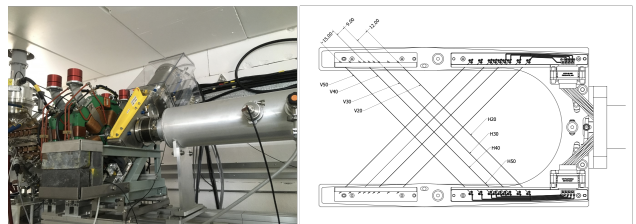


Figure 4: Left: The single WSM on FETS beam line. Right: The monitor head with CNTs. The horizontal wires are upstream of the vertical wires, which are 3 mm apart in the beam direction. The $\phi 10 \mu\text{m}$ CNT was too thin to be mounted on the monitor head.

Figure 5 shows light emission at the wire when interacting with the FETS beam. The smaller the diameter of the wire, the weaker the light emission can be seen at the wire. Based on the beam parameters when the pictures were taken, the steady temperature on the $\phi 20\text{ }\mu\text{m}$ is predicted to be beyond $1000\text{ }^\circ\text{C}$, and the $\phi 20\text{ }\mu\text{m}$ CNT was not broken after at least 10 minutes of exposure to the FETS beam of 28 mA peak current ($3.5\text{E}13$ ppp with a $200\text{ }\mu\text{s}$ pulse). This is a factor of 1×10^3 and 1×10^2 larger than the peak current of the injection pulse (6×10^9 ppp) and the multi-turn accelerating beam (3×10^{11} ppp) in the FETS-FFA ring. Therefore, the considered thickness of CNTs are not expected to be damaged rapidly by the injection beam in the FETS-FFA ring. However, the heat damage over longer durations should also be analysed in future.

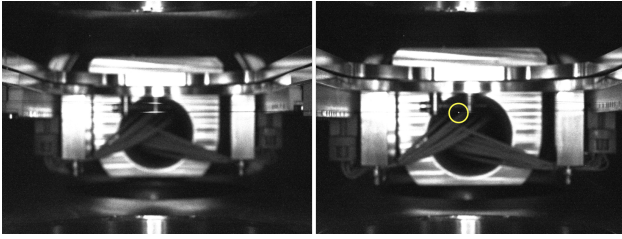


Figure 5: Light emission from the $\phi 50\text{ }\mu\text{m}$ (left) and the $\phi 20\text{ }\mu\text{m}$ (right, in the circle) CNTs with the 3 MeV FETS H^- beam. The wire was aligned at the centre of the beam pipe when the photo was taken.

Pulse Width Measurement on FETS

The pulse width of the FETS beam was measured by the SWIP. The pulse width is determined by the time window which is above 2 times of standard deviation of the noise level. The noise level is found by computing the RMS within a time window at the end of the data when there is no beam. According to the SRIM [13] simulation, the proton range of 3 MeV is expected to be about $120\text{ }\mu\text{m}$ in a Carbon material (1.4 g/cm^3). Therefore, H^- beam will not be fully stopped at the CNTs mounted on the frame, and the electrons of H^- beam will be directly captured by the wire. The negative charge signal is converted to the voltage signal by the operational amplifier and monitored by the oscilloscope. The gain of amplifier is $1 \times 10^3\text{ V/A}$ with 500 kHz frequency bandwidth.

As shown in Fig. 6, the pulse width measured by each CNT wire is within about 5 % different from the one measured by the CT monitor ($210\text{ }\mu\text{m}$) located at about 535 mm upstream of the SWIP. In the integrated signal within the pulse width, the number of primary H^- particles is degraded by about 18 % when it reaches the downstream wires (vertical profile wires in Fig. 6), that agrees with the PHITS [14] simulation. Although the integrated signal was not proportional to the cross-section of the wires, these data will be useful to predict the signal strength when the required diameter of wire is used in the FETS-FFA ring.

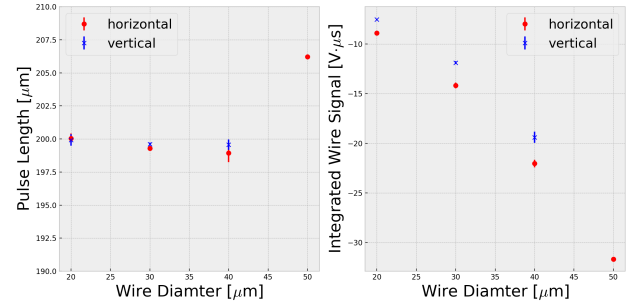


Figure 6: The measured pulse length (left) and the integrated pulse signal (right) of the FETS beam. The error bar is the RMS pulse length and the RMS integrated wire signal over 5 pulses.

BEAM PROFILE MEASUREMENT

Profile Measurement on FETS

The measurement was done by SWIP scanning the wire positions over the beam size. The control units set the wire positions with a stepper motor and acquire the signal at every trigger timing. The control units have a signal amplifier with a gain of $4.7\text{E}3\text{ V/A}$ at bandwidth of 50 kHz after low pass filtering. At each monitor step, 10 samples were acquired over 100 ms following a trigger, and averaged before being saved to disk. As shown in Fig. 7 and Table 2, beam profiles were measured by all CNT wires, and all measured horizontal beam sizes are consistent. The vertical beam sizes are not all consistent, which could be due to scattering from the upstream horizontal profile wires. Based on lattice simulations on the FETS, the RMS beam size at the position of the SWIP is about $4\text{--}5\text{ mm}$. Although the distance between adjacent wires is bigger than the expected beam size, the protons generated at the wires will come in the neighbouring wires, decreasing the signal strength and the signal sensitivity.

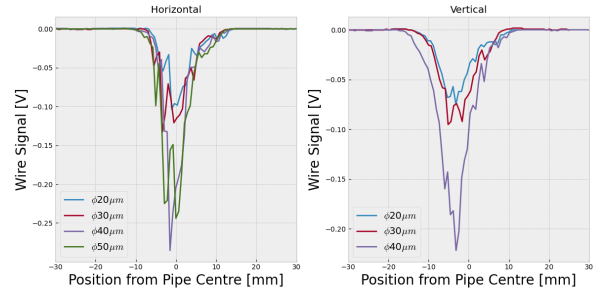


Figure 7: Beam profiles measured by each CNT wire. The scan range was 148.5 mm with a step size of 1 mm . The peak pulse intensity measured by the CT monitor was about 13 mA in this measurement.

Profile Measurement on hFFA

A beam experiment with the single WSM was performed in the hFFA ring at KURNS [15]. The wire position was fixed at the orbit of about 13.5 MeV where the turn separation is about $29\text{ }\mu\text{m}$. A CNT wire with diameter $\phi 10\text{ }\mu\text{m}$ was mounted on the frame as shown in Fig. 8. As the range of 13.5 MeV protons was found to be 1.67 mm in a Carbon

Table 2: The measured RMS beam size with design values. The errors are RMS of three different beam sizes.

CNT	RMS Beam Size Horizontal [mm]	RMS Beam Size Vertical [mm]
$\phi 20 \mu\text{s}$	3.5 ± 0.28	4.2 ± 0.04
$\phi 30 \mu\text{s}$	3.4 ± 0.35	3.8 ± 0.27
$\phi 40 \mu\text{s}$	3.8 ± 0.77	4.6 ± 0.27
$\phi 50 \mu\text{s}$	3.8 ± 0.25	N.A.
Design	4-5	4-5

material (1.4 g/cm^3) by SRIM simulation, the protons were expected to be fully stopped at the CNT wire. Therefore, secondary electron emissions were read by the signal amplifier with a gain of $1 \times 10^7 \text{ V(A)}$ and a cutoff frequency of 4.8 kHz that was wide enough to detect the $\approx 300 \mu\text{s}$ beam signal.

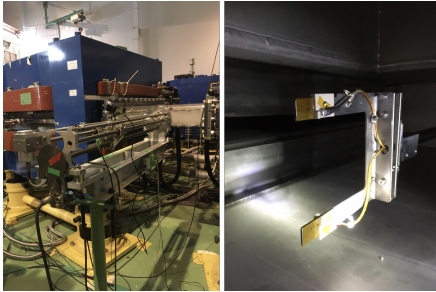


Figure 8: The radial probe (left) and the monitor head of the single WSM with $\phi 10 \mu\text{m}$ CNT wire (right). The monitor head was attached to the radial probe and controlled by the motion control driver.

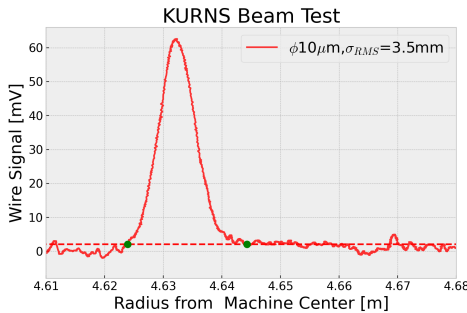


Figure 9: The accelerating multi-turn beam profile measured by a $\phi 10 \mu\text{m}$ CNT wire. The dashed line indicates 2 times of standard deviation of the noise level, computed by the RMS within a time window at the end of the data when there is no beam.

Although the shape of beam profile is similar between the measurement (Fig. 9) and the simulation (Fig. 10) based on the KURNS ring optics and the beam parameters, the measured beam size is smaller than that of design value. The injector (11 MeV H^- Linac) was not stable during the experiment, and the ion source as well as following beam transports were recommissioned prior to the tests. Discrepancies between measurement and expectation could possibly be explained by differences between the actual and design beam emittance.

Stray magnetic fields from the main hFFA magnets is close to 0.05 T near the middle of the straight section where the single WSM was installed. Based on CST tracking simulations [16], some of the secondary electrons generated at the wire will be confined by the magnetic fields and eventually return to the wire, decreasing the signal and resulting in a smaller measured beam size. Profile measurements with a negative bias voltage were planned, but not performed due to time constraints.

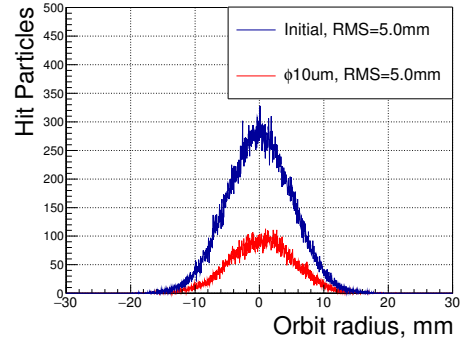


Figure 10: The computed beam profile measured by $\phi 10 \mu\text{m}$ wire. The initial beam is a Gaussian distribution with the design value of beam size ($\sigma = 5 \text{ mm}$). The scattering angle and energy loss at the wire are computed by PHITS, which are taken into account in this simulation.

CONCLUSION

The WSM with a single, stationary CNT wire has been developed as a beam profile monitor for the FETS-FFA test ring. Tracking simulations have motivated the study of wires with a small diameter, to minimise scattering over many turns. The durability of these wires has been demonstrated by exposing them to the 3 MeV H^- beam of the FETS Linac. Whilst it has been demonstrated with simulations and measurements that heating of these wires is not expected to produce short-term effects, heat damage over a longer time periods should be also observed in future. It has also been demonstrated with simulations and experimentally, that the single WSM will be able to measure the pulse length and profile of low energy mono-energetic beams as well as the accelerating beam over multiple turns in the FETS-FFA ring. A beam scraper will also be installed in the FETS-FFA ring, and offers an alternative method to measure the beam size of accelerating beams over multiple turns. However, there are challenges in using such monitors when distributions such as hollow beams are possible. As the single WSM will be able to identify the beam profile and the beam size even for a hollow beam, the single WSM will be an invaluable diagnostic for commissioning the FETS-FFA test ring.

ACKNOWLEDGEMENTS

The author wishes to acknowledge the efforts by S. Kellard and A. Chamberlain for the design and manufacture of the single WSM.

REFERENCES

- [1] J.-B. Lagrange *et al.*, “Progress on Design Studies for the ISIS II Upgrade”, in *Proc. IPAC’19*, Melbourne, Australia, May 2019, pp. 2075–2078.
doi:10.18429/JACoW-IPAC2019-TUPTS068
- [2] T. Ohkawa, “Proc. Annual meeting of JPS”, 1953, unpublished.
- [3] K. R. Symon *et al.*, “Fixed-Field Alternating-Gradient Particle Accelerators”, *Phys. Rev.*, vol. 103, pp. 1837–1859, 1956.
doi:10.1103/PhysRev.103.1837
- [4] HiTaCa by Hitachi Zosen Ltd.,
<https://www.hitachizosen.co.jp/>
- [5] DexMat, <https://store.dexmat.com/>
- [6] A. Miura, K. Moriya, and T. Miyao, “Application of Carbon Nanotube Wire for Beam Profile Measurement of Negative Hydrogen Ion Beam”, in *Proc. IPAC’18*, Vancouver, Canada, Apr.-May 2018, pp. 5022–5025.
doi:10.18429/JACoW-IPAC2018-FRXGBD3
- [7] J.-B. Lagrange *et al.*, “FETS-FFA Ring Study”, in *Proc. IPAC’21*, Campinas, Brazil, May 2021, pp. 1901–1904.
doi:10.18429/JACoW-IPAC2021-TUPAB208
- [8] S. Machida *et al.*, “Internal Report for FFA Task Report vFFA”, 2022, unpublished.
- [9] R. Calaga *et al.*, “PYTRACK: self-developed particle transport code”, unpublished.
- [10] D. W. Posthuma de Boer and A. Pertica, “Thermal Simulations of Wire Profile Monitors in ISIS Extracted Proton Beamline 1”, in *Proc. IBIC’16*, Barcelona, Spain, Sep. 2016, pp. 785–787. *doi*:10.18429/JACoW-IBIC2016-WEPG59
- [11] A. P. Letchford, “Upgrades and Developments at the ISIS Linac”, in *Proc. LINAC’22*, Liverpool, UK, Aug.-Sep. 2022, pp. 1–6. *doi*:10.18429/JACoW-LINAC2022-M01AA01
- [12] D. M. Harryman and C. C. Wilcox, “An Upgraded Scanning Wire Beam Profile Monitoring System for the ISIS High Energy Drift Space”, in *Proc. IBIC’17*, Grand Rapids, MI, USA, Aug. 2017, pp. 396–400.
doi:10.18429/JACoW-IBIC2017-WEPCC18
- [13] J. F. Ziegler, M. D. Ziegler and J. P. Biersack, “SRIM - The Stopping and Range of Ions in Matter”, *Nucl. Instrum. Methods Phys. Res., Sect. B*, vol. 268, no. 11, pp. 1818–1823, 2020.
doi:10.1016/j.nimb.2010.02.091
- [14] T. Sato *et al.*, “Features of Particle and Heavy Ion Transport code System (PHITS) version 3.02”, *J. Nucl. Sci. Technol.*, vol. 55, no. 6, pp. 684–690, 2018.
doi:10.1080/00223131.2017.1419890
- [15] Y. Mori *et al.*, “Present Status of FFAG Proton Accelerator at KURRI”, in *Proc. IPAC’11*, San Sebastian, Spain, Sep. 2011, paper WEPS077, pp. 2685–2687.
- [16] CST Studio Suite: Electromagnetic field simulation software, <https://www.3ds.com/products-services/simulia/products/cst-studio-suite/>